Dynamic Shape of the Depletion Layer of a Submillimeter-Wave Schottky Varactor

Jyrki T. Louhi and Antti V. Räisänen, *Fellow, IEEE*

Abstract—**Most frequency multipliers at submillimeter wavelengths are based on the Schottky varactor. The main problem of these multipliers is the output power, which remains low at frequencies above 500 GHz. The aim of this work is to help the situation by studying the usability of the conventional equivalent circuit during a fast voltage modulation. The anode edge effects play an important role in this voltage modulation. While the fringing fields, due to the edge effects, reduce the capacitance modulation in small submillimeter-wave varactors, the edge effects also lessen the effect of electron velocity saturation compared with an ideal varactor with a pure parallel plate capacitance. The usefulness of the static model can be estimated by comparing the three-dimensional shape of the depletion layer to the shape given by the dynamic model. The dynamic shape can be obtained by solving the potential and electron conduction currents in the epitaxial layer of the Schottky varactor. In this work the potential and the electron currents have been calculated from simplified device physics by using numerical methods.**

I. Introduction

FREQUENCY multipliers are used to generate the all-solid-state local oscillator power of heterodyne receivers at millimeter and submillimeter wavelengths [1]. These local oscillators are needed in many future scientific satellites (e.g., SWAS, Odin and FIRST) and atmospheric limb sounders (e.g., MASTER and SOPRANO). At millimeter and submillimeter wavelengths a Schottky varactor is the most commonly used multiplier device, although several novel varactors (SBV, QWD, BNN, bbBNN, HEMV) have been proposed [2]. The main problem of the submillimeter-wave frequency multiplier is the output power, which is low at frequencies above 500 GHz, although some promising work has recently been carried out at frequencies near 1 THz [3], [4].

The conventional equivalent circuit of the submillimeter-wave Schottky varactor consists of a nonlinear junction capacitance, a nonlinear junction conductance, a series impedance, and a model for electron velocity saturation [1], [5]. The aim of this work is to study the usability of the equivalent circuit, especially the usefulness of the model used for edge effects during fast voltage modulation. While the fringing fields, due to the edge effects, reduce the capacitance modulation in every submillimeter-wave Schottky varactor, the edge effects also affect the electron velocity saturation. This makes it important to carefully analyze the behavior of the edge effects. We have approached this task by analysing the three-dimensional (3-D) dynamic shape of the depletion layer of a small-area Schottky varactor. The usefulness of the conventional equivalent circuit can be found by comparing the calculated dynamic shape of the depletion layer to the solution obtained by employing a static model. More detailed information can be found by calculating the junction capacitance during the fast voltage modulation and by comparing it with the static capacitance. The problem is rather complicated and therefore simplified device physics must be employed to get even the basic information about the dynamic shape of the depletion layer.

Manuscript received June 29, 1995; revised August 26, 1996.

The authors are with the Radio Laboratory, Helsinki University of Technology, FIN-02150 Espoo, Finland.

Publisher Item Identifier S 0018-9480(96)08482-7.

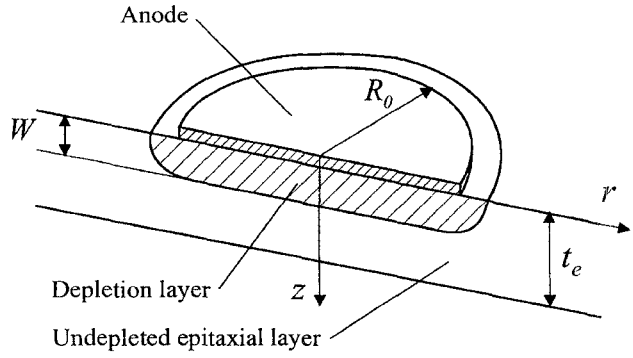

Fig. 1. Cross section of the Schottky varactor.

II. Formulation of the Problem

A circular metallic anode is assumed to be at the top of the epitaxial semiconductor (GaAs), as shown in Fig. 1. The radius of the anode is R_0 and the thickness of the epitaxial layer is t_e. The approximate shape of the depletion layer is also shown in Fig. 1, when the anode is charged to a static potential $\phi_0 = V - \phi_{bi}$.

In the static situation, the electric equilibrium is reached and no current is flowing in the epitaxial layer (except the equal numbers but opposite signs of drift and diffusion currents, in the transition between the undepleted and depleted layers). When the potential of the anode is increased (or decreased), the potential of the epitaxial layer has to change, which means that drift current begins to flow in the undepleted layer. The current moves the transition front. If the potential of the anode is increased very slowly, the 3-D shape of the transition front during the transient is equal to the front obtained using the static solution. If the potential is increased fast enough, however, the shape of the transition front is affected by the electron velocity saturation as well as by the edge effects due to the circular anode.

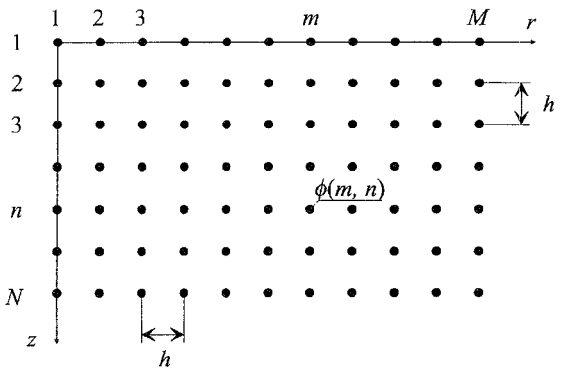

Fig. 2. Mesh used in simulations.

The behavior of the transition front during the fast voltage modulation can be analyzed in three different ways.

1) The most physical way is to use the drift-diffusion model with energy balance equations [6], [7]. The results obtained in this way are exact, but the physical model as well as the computer routines required to carry out either 3-D or two-dimensional (2-D) analyses are intricate.
2) A moderate way is to employ simplified device physics. This means that components that have a negligible effect on the results are removed from the complete drift-diffusion model.
3) The easiest way to analyze the behavior of the transition front is to assume that the transition front is only slightly affected, due the fast voltage modulation. This assumption means that there is no need to change the model obtained by using static equations [5].

Because the first way is complicated, we have employed the simplified device physics (second choice) to get the basic information considering the shape of the transition front during the fast voltage modulation. The main reason for using the simplified device physics is to reduce the computing time required in analyses. Compared with the drift-diffusion model [6], the simplified device physics includes the following assumptions.

1) Although the Debye length L_D is not negligible, we have assumed the transition front between the depleted and undepleted layers to be abrupt. This assumption can be done because the distribution of the free electrons in the transition front does not change when the transition front is moving during a voltage sweep.
2) Because the effect due to the net charge recombination is small, we have assumed the recombination to be zero.
3) Because the Schottky varactors are heavily n-doped, the currents due to holes are negligible.

To further simplify the analyzes the following assumptions considering the problem geometry and boundary conditions are made.

1) Because the conductivity of the substrate is much greater than the conductivity of the epitaxial layer, the substrate layer is assumed to be a perfect conductor and, therefore, the potential of the substrate layer is zero.
2) Because the permittivity of GaAs is greater than the permittivity of air, the normal component of the electric field is assumed to be zero in the air-GaAs interface.
3) The radius of the epitaxial layer is assumed to be four times the radius of the anode. This decreases the time required in numerical analyses compared with the case when the real radius of the epitaxial layer is employed. This assumption can be made because the potential strongly decreases when the distance from the axis of the cylindrical epitaxial layer increases. The potential is negligible at the distance of two to three times R_0 away from the axis.

The above assumptions must be traded against the decreased complexity of the problem as well as the decreased time required in the numerical simulations.

III. Simplified Device Equations

A. Poisson's Equation

The potential ϕ in the epitaxial layer can be found by using Poisson's equation [8]

$$\nabla^2\phi = -\frac{\rho}{\epsilon} \tag{1}$$

where ρ is the net volume charge density and ϵ is the permittivity. The electric field is

$$\vec{\mathcal{E}} = -\nabla\phi \tag{2}$$

and the net volume charge density is

$$\rho = q(N_D - n) \tag{3}$$

where q is the charge of the electron and N_D is the doping density. When the transition front is assumed to be abrupt, the density of free electrons in the undepleted layer is equal to N_D and therefore the net volume charge is zero. In the totally depleted layer, the density of free electrons is zero and the net charge per unit volume is equal to qN_D.

B. Current Density

The electron current density is the sum of the drift and diffusion components [6], [7]

$$\vec{J}_n = q\mu(\mathcal{E})n\vec{\mathcal{E}} + qD_n\nabla n \tag{4}$$

where $\mu(\mathcal{E})$ is the electron mobility and the diffusivity D_n is given by the Einstein relation

$$D_n = \frac{kT}{q}\mu(\mathcal{E}). \tag{5}$$

When the transition layer front is assumed to be abrupt, the density of free electrons in the depleted layer is zero and, therefore, the electron current is also zero. In the undepleted layer, the density of free electrons is constant N_D and, therefore, the electron current density is

$$\vec{J}_n = q\mu(\mathcal{E})N_D\vec{\mathcal{E}}. \tag{6}$$

When the transition front is assumed to be abrupt, the diffusion current is always zero. In reality, the diffusion current affects the density of free electrons near the transition layer. The diffusion current does not, however, affect the movement

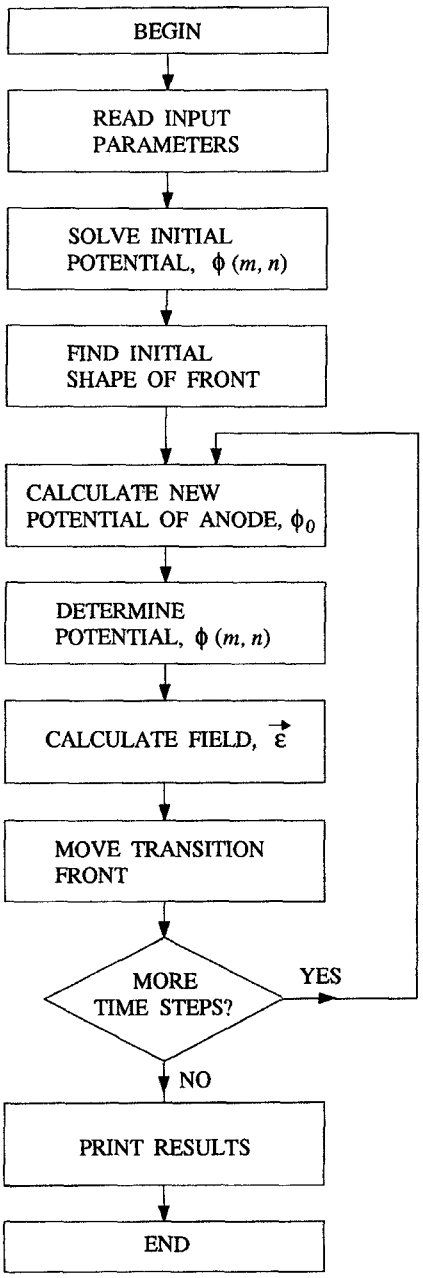

Fig. 3. The computer algorithm.

of the transition front and therefore the assumption of an abrupt transition can be made.

The continuity equation for the electron current density is

$$\nabla \cdot \vec{J}_n - q\frac{\partial n}{\partial t} = 0. \tag{7}$$

By employing (6) and (7), the velocity of the transition front can be derived to be

$$\vec{v} = -\mu(\mathcal{E})\vec{\mathcal{E}}. \tag{8}$$

IV. Numerical Method

A. Algorithm

Because the problem cannot be solved by using analytical methods, the effect of the voltage modulation on the shape of the transition front has been studied by using a numerical

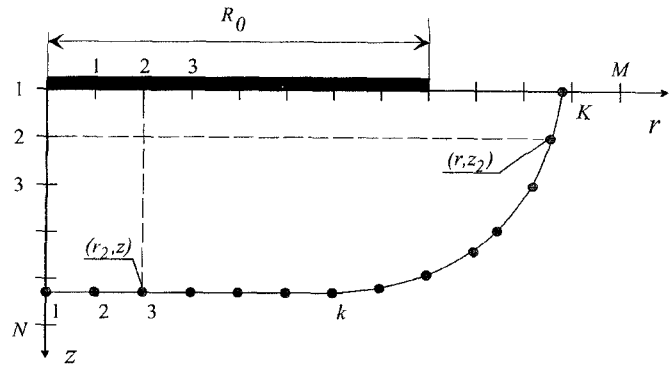

Fig. 4. Corner points of the transition front.

method (in 2-D because of cylindrical symmetry). Poisson's equation has been solved numerically by using the finite difference method, where the epitaxial layer is divided into a dense mesh of size $M \times N$ as shown in Fig. 2. The potential of each mesh point $\phi(m, n)$ is determined by using the discrete Poisson's equation and the iterative over-relaxation method [9], [10].

The transition front between the depleted and undepleted layers has been modeled by using discrete corner points as shown in Fig. 4. The corner points are moved according to the electric field, which is calculated from the potential by using a numerical version of equation (2). The net volume charge of each mesh point is determined according to the information of the corner points. If the mesh point is inside the transition front (depleted layer) the net volume charge is N_D; otherwise (undepleted layer) the charge is zero at the mesh point.

The computer algorithm of the simulation program is shown in Fig. 3. At the beginning of the simulation, the potential of the epitaxial layer is determined by using a numerical method described in [9] and [10]. Then the initial shape of the transition front is determined from this numerically solved potential. The discrete corner points of the transition front are placed smoothly over the transition front so that the vertical (or horizontal) spacing between corner points is equal to the spacing of the initial mesh as shown in Fig. 4.

At the beginning of each time step, the potential of the anode is determined according to the input parameters of the program. Then the net volume charge of each mesh point is determined from the shape of the transition front (charge is zero in the undepleted layer and equal to qN_D in the depleted layer). After that, the potential of each mesh point is calculated numerically by using the iterative over-relaxation method. When the potential is known, the electric field is found by using a numerical version of (2). Finally, the corner points of the transition front are moved according to the electric field. The movement of the corner point is given by

$$\Delta s = -\mu(\mathcal{E}_n)\mathcal{E}_n \Delta t \tag{9}$$

where Δt is the time step and $\mathcal{E}_n$ is the normal component of the electric field at the corner point. In simulations we have used a simple expression for the velocity versus field, which has a constant mobility ($\mu = 0.55$ m^2/Vs) at low fields and a constant maximum velocity ($v_m = 2.9 \times 10^5$ m/s) at higher fields.

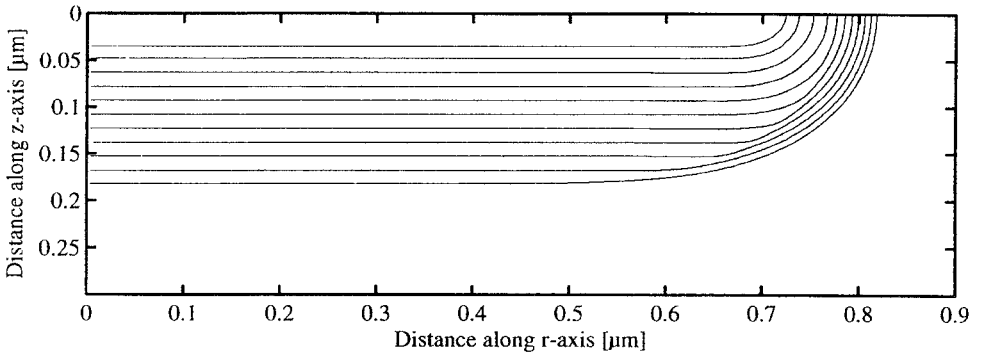

Fig. 5. The shape of the transition front during a negative voltage ramp.

B. Junction Capacitance

Because the shape of the depletion layer during a voltage modulation differs from that obtained by using the static equations [10], the junction capacitance during a transient must be determined by using the net charge of the depletion layer. The net charge can be calculated by using information about the corner points and it is given by the numerical equation

$$Q_{\text{tot}} = qN_D \sum_{k=2}^{K} 2\pi \frac{r_k + r_{k-1}}{2} \frac{z_k + z_{k-1}}{2} (r_k - r_{k-1}) \quad (10)$$

where r_k and z_k are the coordinates of the corner point k. The junction capacitance at the time step t is given by

$$C_j = \frac{\Delta Q}{\Delta V_j} = \frac{Q_{t+1} - Q_{t-1}}{V_{t+1} - V_{t-1}} \quad (11)$$

where Q_t is the net charge of the depletion layer at the time step t and V_t is the voltage over the depletion layer.

V. Results

The simulation program can be used to analyze any millimeter or submillimeter-wave Schottky varactor. Because the time required to analyze the varactor during a single pump cycle is very long (about 20 h for Cray C94), the program cannot be directly integrated with the harmonic balance method. For that reason, we have first analyzed the varactor during a linear voltage sweep, which is a good approximation for the modulation of the anode voltage, when the charge of the depletion layer is loaded or unloaded during the pump cycle. After that we have analyzed the varactor by using a more realistic waveform, which is obtained by using the harmonic balance method [11] with the conventional model.

Because the effect of the voltage modulation depends on the parameters of the varactor as well as on the frequencies and power levels of the multiplier, the actual shape of the depletion front must be analyzed separately for each case. As an example, we have analyzed a very small area Schottky varactor, the parameters of which are given in Table I.

TABLE I
Parameters of the Schottky Varactor for 1-THz Range

Radius of the anode	R_0	0.7	μm
Thickness of the epitaxial layer	t_e	0.2	μm
Doping density	N_D	$1.0 \cdot 10^{17}$	cm^{-3}
Series resistance	R_s	12	Ω
Junction capacitance at zero bias	C_0	1.8	fF

A. Linear Voltage Sweep

We have first analyzed the varactor during a simple negative voltage sweep (from positive to negative voltage). At the beginning of the simulated negative sweep, the applied voltage V is slightly smaller than the contact potential ϕ_{bi}. During the simulation, the potential of the anode has been decreased by 5 mV/fs. The total time of the voltage sweep is 0.5 ps, which is one half of the cycle at the frequency of 1 THz. The transition front between the depleted and undepleted layer is shown in Fig. 5, where the time difference between two fronts is 50 fs. At the beginning of the negative sweep, the epitaxial layer is almost totally undepleted and the shape of the transition front is equal to the shape that can be obtained by static equations. When the currents begin to flow in the epitaxial layer, the volume of the depleted layer increases. Because the potential of the anode is decreased very fast, the electric field in the epitaxial layer is high and so the transition front moves with the maximum velocity of electrons. The electric field is extremely high near the edge of the anode, which means that the transition front moves there with the maximum, saturated velocity of electrons. Now the shape of the transition front is almost equal to the shape of a quarter of a circle as shown in Fig. 5. This means that the volume of the depletion layer increases faster than can be assumed by using static equations. At the end of the negative sweep, the velocity of the transition front near the center of the anode is still equal to the maximum velocity of electrons. Near the edge of the anode the velocity of the transition front decreases, however, because the electric field decreases as the distance from the edge of the anode increases. This means that at the end of the sweep the increase of the net charge is slower than can be assumed by using static equations.

We have also analyzed the varactor in an opposite case, during a positive voltage sweep (from negative to positive voltage). The transition front during the positive sweep is shown in Fig. 6. At the beginning of the positive, sweep the epitaxial layer is almost totally depleted and the shape of the transition front is equal to the shape which can be obtained by static equations. When the currents begin to flow, the volume of the depletion layer decreases. Even though the voltage of the anode is now increased with the same speed as it is decreased in the opposite case, the velocity of the transition front does not saturate at the beginning of the sweep. This can be understood,

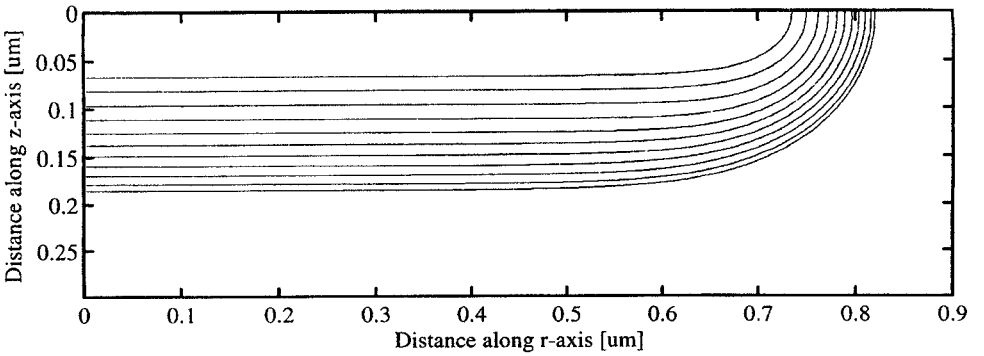

Fig. 6. The shape of the transition front during a positive voltage ramp.

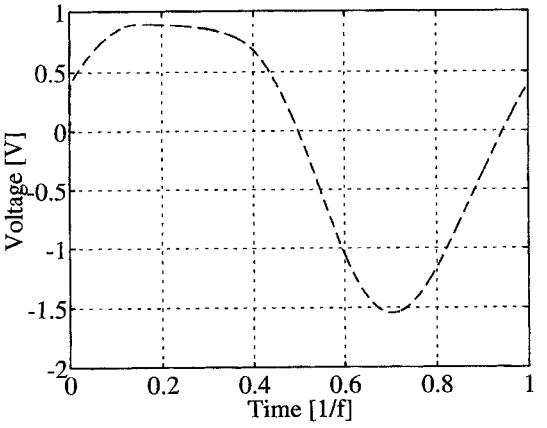

Fig. 7. Voltage waveform of a doubler for 1 THz with input power of 2 mW.

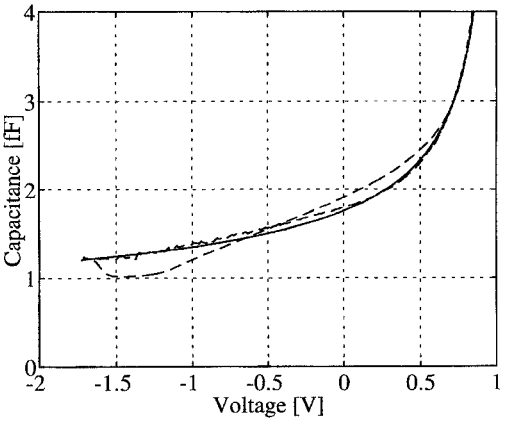

Fig. 8. The capacitance of the varactor. The solid line is obtained with static equations and the dashed line with a numerical solution using a 1-THz sweep.

because the junction capacitance is now smaller than at the beginning of the negative voltage sweep, which means that the required current is also smaller. Therefore, at the beginning of the positive voltage sweep, the shape of the transition front is equal to the shape obtained by static solution. At the end of the positive sweep, however, the electric field is high enough and the velocity of the transition front saturates as shown in Fig. 6. At the same time, the shape of the transition front differs from the shape obtained by static equations. In this case, the behavior of the transition front is same as that at the beginning of the negative sweep. The shape of the transition front during the entire negative and positive voltage sweeps, however, are not identical; some kind of hysteretic behavior is taking place.

B. Pumped Varactor

The actual behavior of the small area submillimeter-wave Schottky varactor should be analyzed by integrating the new routine with the harmonic balance method. Because the time required to analyze a single pump cycle is long, the new routine cannot be directly integrated with the harmonic balance method. Quite realistic results can be obtained, however, if the voltage waveform is first calculated by employing the harmonic balance method with the conventional varactor model and then this waveform is used in the new routine. The corrected $C-V$ characteristic and electron velocity saturation model obtained are then used in the harmonic balance analysis in order to simulate the multiplier.

As an example, we have analyzed a Schottky varactor as a doubler (2×500 GHz) by employing first the equivalent circuit presented in [5] with the harmonic balance method [11]. The voltage waveform of the doubler for 1 THz is shown in Fig. 7 (input power is 2.0 mW). The voltage form includes three different kinds of areas: 1) a constant voltage area (applied voltage is from 0.75 to 0.9 V); 2) negative voltage sweep area (applied voltage decreases from 0.75 V to -1.5 V); and 3) positive voltage sweep area (applied voltage increases from -1.5 V to 0.75 V). By applying this voltage waveform over the varactor, the following observations are made when using the new numerical model. During the constant voltage, the epitaxial layer is almost totally undepleted and the shape of the depletion layer is equal to the shape obtained by the static model. During the negative sweep area, however, the shape of the depletion layer differs from the shape obtained by the static model. In this case, the behavior of the depletion layer shape is rather similar to the shape that is obtained by employing a linear negative voltage sweep. During the positive sweep, the velocity of the depletion layer front is always smaller than the maximum velocity of electrons and, therefore, the shape of the depletion layer is almost identical to the static shape. This means that shape of the depletion layer during the negative and positive voltage sweeps are different.

The calculated capacitance of the varactor during a 1-THz voltage sweep is shown in Fig. 8. During the constant voltage area, the numerically obtained junction capacitance is equal to the static capacitance. This can be understood, because

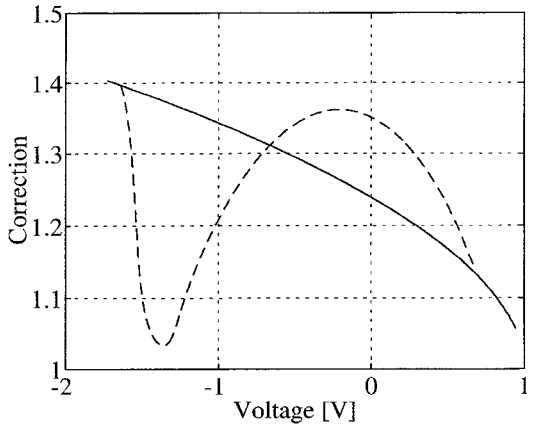

Fig. 9. The correction factor γ_C of the varactor. The solid line is obtained with static equations and the dashed line with a numerical solution.

the applied voltage is almost constant or it changes very slowly and so the shape of the depletion layer is equal to the shape obtained by employing the static methods. During the negative sweep, the capacitance differs from the capacitance obtained by employing the static equations. At the beginning of the negative sweep (applied voltage decreases from 0.75 V to −0.5 V), the volume of the depletion layer increases faster than can be assumed by the static equations, and so the dynamic capacitance is larger than the static capacitance. At the end of the negative voltage sweep (applied voltage decrease from −0.5 V to −1.5 V), the volume of the depletion layer increases slowly and the dynamic capacitance is smaller than the static capacitance. During the positive sweep, the dynamic capacitance is equal to the static capacitance. This means that according to our simulations, the capacitance of the Schottky varactor has hysteretic behavior under rapid pumping.

At submillimeter wavelengths, the maximum output power of the Schottky varactor frequency multiplier is strongly affected by the electron velocity saturation [12]. The saturation effect can be included in the static model of the varactor by limiting the electron conduction current to the value of the maximum current [5]

$$i_{\max} = AN_D q v_m \gamma_C \tag{12}$$

where v_m is the maximum velocity of electrons. In the dynamic case, the net correction factor γ_C can be calculated from the numerically obtained capacitance. The behavior of the net correction factor during the pump cycle is shown in Fig. 9. As shown in the figure, at the beginning of the negative voltage sweep the numerically obtained correction factor is larger than the static value. At the end of the negative voltage sweep, however, the numerically obtained correction factor is small. This means that at the beginning of the negative voltage sweep the electron conduction current may be much larger than can be assumed by using static equations. This helps to pump the varactor more effectively. During the positive voltage sweep, the numerically obtained junction capacitance is equal to the static capacitance and so the correction factor is also equal to the value obtained by using the static model.

The efficiency of the entire frequency multiplier circuit increases slightly (less than 1 dB), when the above dynamic model is employed instead of the conventional static model including the model for electron velocity saturation. The increase is mainly due to the increased maximum current of the varactor. The effect is, however, much smaller than the effect due to the electron velocity saturation. This means that the conventional model including the model for electron velocity saturation can be employed in most cases.

VI. Conclusion

The equivalent circuit of the submillimeter-wave Schottky varactor is strongly affected by edge effects. While edge effects reduce the capacitance modulation, they also lessen the effect of electron velocity saturation. In this work, we have studied the usefulness of the conventional model used for edge effects by analysing the three dimensional shape of the transition front between the depleted and undepleted layer. According to our results, the shape of the transition front in a small area Schottky varactor is affected by the fast voltage modulation during the pump cycle of a submillimeter wave frequency multiplier. When the new dynamic model is employed, the calculated efficiency of the entire frequency multiplier circuit increases slightly compared with results obtained by the conventional static model, including the model for electron velocity saturation. The difference is much smaller, however, than the difference obtained by employing the conventional models with and without the model for electron velocity saturation. Therefore, in most practical cases the submillimeter-wave Schottky varactor can be analyzed, designed, and optimized by employing the previously obtained model [5]. If the Schottky varactor is to be analyzed very carefully, however, the dynamic model should be employed.

References

[1] A.V. Räisänen, "Frequency multipliers for millimeter and submillimeter wavelengths," *Proc. IEEE*, vol. 80, no. 11, pp. 1842–1852, 1992.
[2] M. A. Frerking and J. R. East, "Novel heterojunction varactors," *Proc. IEEE*, vol. 80, no. 11, pp. 1853–1860, 1992.
[3] R. Zimmermann, T. Rose, and T. Crowe, "An all solid-state 1 THz radiometer for space applications," in *Proc. 6th Int. Symp. Space Terahertz Technology*, Pasadena, CA, 1995, pp. 13–27.
[4] N. Erickson and J. Tuovinen, "A waveguide tripler for 800–900 GHz," in *Proc. 6th Int. Symp. Space Terahertz Technology*, Pasadena, CA, 1995, pp. 191–198.
[5] J. T. Louhi and A. V. Räisänen, "On the modeling and optimization of Schottky varactor frequency multipliers at submillimeter wavelengths," *IEEE Trans. Microwave Theory Tech.*, vol. 43, no. 4, pp. 922–926, 1995.
[6] T. Adachi, A. Yoshii, and T. Sudo, "Two-dimensional semiconductor analysis using finite element method," *IEEE Trans. Electron Devices*, vol. ED-26, no. 7, pp. 1026–1031, 1979.
[7] H. Hjelmgren, "Numerical modeling of hot electrons in n-GaAs Schottky-barrier diodes," *IEEE Trans. Electron Devices*, vol. 37, no. 5, pp. 1228–1234, 1990.
[8] S. M. Sze, *Physics of Semiconductor Devices*. New York, Wiley, 1981.
[9] E. Wasserstrom and J. McKenna, "The potential due to a charged metallic strip on a semiconductor surface," *Bell Syst. Tech. J.*, pp. 853–877, May–June 1970.
[10] J. T. Louhi, "The capacitance of a small circular Schottky diode for submillimeter wavelengths," *IEEE Microwave Guided Wave Lett.*, vol. 4, no. 4, pp. 107–108, 1994.
[11] P. H. Siegel, A. R. Kerr, and W. Hwang, "Topics in the optimization of millimeter—Wave mixers," NASA Tech. Paper 2287, 1984.
[12] E. L. Kollberg, T. J. Tolmunen, M. A. Frerking, and J. R. East, "Current saturation in submillimeter wave varactors," *IEEE Trans. Microwave Theory Tech.*, vol. 40, no. 5, pp. 831–838, 1992.

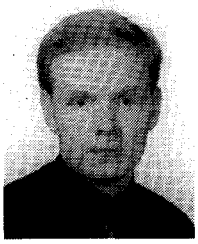

Jyrki T. Louhi was born in Sauvo, Finland, on September 12, 1967. He received the degree of the Diploma Engineer (M.Sc.) with honors and the Licentiate of Technology degree in electrical engineering from Helsinki University of Technology (HUT), Espoo, Finland, in 1991 and 1994, respectively. He is currently working toward the Ph.D. degree.

Since 1991, he has been a Research Engineer as well as a Teaching Assistant at the Radio Laboratory HUT. His research interests lie in the submillimeter-wave heterodyne receivers, mixers, and frequency multipliers.

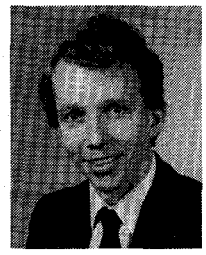

Antti V. Räisänen (S'76–M'81–SM'85–F'94) was born in Pielavesi, Finland, on September 3, 1950. He received the Diploma Engineer (M.Sc.), the Licentiate of Technology, and the Doctor of Technology degrees in electrical engineering from Helsinki University of Technology (HUT), Finland, in 1973, 1976, and 1981, respectively.

From 1973 to 1978, he was a Research Assistant at HUT Radio Laboratory. From 1978 to 1979, he was a Research Assistant at Five College Radio Astronomy Observatory (FCRAO) of the University of Massachusetts, Amherst. From 1980 to 1983, he was a Research Fellow of the Academy of Finland, working mainly at HUT, but also for shorter periods at FCRAO and Chalmers University of Technology, Gothenburg, Sweden. In 1984, he was a Visiting Scientist at the Department of Physics, University of California, Berkeley. From 1985 to 1989, he was an acting Professor of Radio Engineering with HUT, working also for short periods at the UC-Berkeley. In 1989, he was appointed by invitation to the Professor Chair of Radio Engineering with HUT. In 1992 and 1993 he was on sabbatical leave from HUT and had a Senior Research Fellowship from the National Research Council at the Jet Propulsion Laboratory, Pasadena, CA. He was also a Visiting Associate in Electrical Engineering at the California Institute of Technology, Pasadena. He is supervising research in millimeter components, antennas and receivers, microwave propagation in satellite links, microwave measurements, etc. at HUT Radio Laboratory. He has authored and co-authored more than 200 scientific or technical papers and three books: *Microwave Measurement Techniques Radio Engineering, and RF and Microwave Techniques* (Finland: Otatieto, 1991, 1992, and 1994, respectively, all in Finnish).

Dr. Räisänen was the Secretary of the 12th European Microwave Conference (1982). He was the Counselor of the IEEE Student Branch in Helsinki from 1982 to 1989 and the Chairman of the IEEE MTT/AP Chapter in Finland from 1987 to 1992. In 1992, he served as the Conference Chairman for the 22nd European Microwave Conference. Currently, he serves in the Research Council for Natural Sciences and Engineering, the Academy of Finland.